ELSEVIER

Computers and Geotechnics 23 (1998) 237–253

COMPUTERS AND GEOTECHNICS

Effective width rule in calculations of bearing capacity of shallow footings

Radoslaw L. Michalowski *, Liangzhi You

Department of Civil Engineering, The Johns Hopkins University, Baltimore, MD 21218, USA

Received 23 April 1998; received in revised form 25 August 1998; accepted 14 October 1998

Abstract

The classical solution to the bearing capacity problem predicts the limit load on symmetrically loaded shallow strip footings. A useful hypothesis was suggested by Meyerhof to account for eccentricity of loading, in which the footing width is reduced by twice-the-eccentricity to its 'effective' size. This hypothesis sometimes has been criticized as being overconservative. This paper examines Meyerhof's suggestion and presents the bearing capacity of eccentrically loaded footings calculated using the kinematic approach of limit analysis. It is found that the effective width rule yields a bearing capacity equivalent to that calculated based on the assumption that the footing is smooth. For more realistic footing models and for cohesive soils the effective width rule is a reasonable account of eccentricity in bearing capacity calculations. Only for significant bonding at the soil-footing interface and for large eccentricities does the effective width rule become overly conservative. For cohesionless soils, however, the effective width rule may overestimate the best upper bound. This overestimation increases with an increase in eccentricity.

1. Introduction

Classical solutions to the bearing capacity problem (Prandtl [1] and Reissner [2]) assume that the load applied to the footing is symmetric. Eccentricity of the load is commonly included in design by reducing the width of the footing, B, by twice-the-eccentricity, $2e$, thus reducing the effective width to $B-2e$. This approach was suggested by Meyerhof [3], and it has been widely accepted in geotechnical design. This procedure is referred to here as the *effective width rule*. The issue was raised in the literature that the procedure is conservative for cohesive soils, and that it may overestimate the bearing capacity for frictional soils (for instance, Pecker and Salençon

* Corresponding author. Fax: +1-410-516-7473; e-mail: rlm@jhu.edu

0266-352X/99/$—see front matter
PII: S0266-352X(98)00024-X

[4]). The aim of this paper is to obtain a limit analysis solution to eccentrically loaded strip footings, and to assess the effective width rule and interpret it in terms of plasticity analysis. The kinematic approach of limit analysis will be used to solve the bearing capacity problem of a footing subjected to eccentric loading. This approach is based on a theorem which, for a perfectly plastic associative material, states that *the rate of work dissipation is not less than the rate of work of external forces for any kinematically admissible collapse mechanism*. This can be written as

$$\int_V \dot{D}(\dot{\varepsilon}_{ij})\mathrm{d}V \geq \int_{S_v} T_i v_i \mathrm{d}S_v + \int_{S_t} T_i v_i \mathrm{d}S_t + \int_V \gamma_i v_i \mathrm{d}V \tag{1}$$

where $\dot{D}(\dot{\varepsilon}_{ij})$ is the rate of work dissipation during incipient failure, and T_i is the stress vector on boundaries S_v and S_t. Vector T_i is unknown (limit load) on S_v and known on S_t (for instance, surcharge pressure). v_i is the velocity vector field in the kinematically admissible mechanism, γ_i is the specific weight vector, and V is the volume of the mechanism.

For a translational mechanism, where the footing (boundary S_v) moves as a rigid body (but does not rotate), the first integral on the right-hand side of Eq. (1) can be written as $v_i \int T_i \mathrm{d}S_v$, and an upper bound to the total unknown limit load (bearing capacity) $\int T_i \mathrm{d}S_v$ can be calculated from Eq. (1). Now it becomes apparent that a solution to the total limit load, based on a translational mechanism, is independent of eccentricity, since the work rate of the limit load, $v_i \int T_i \mathrm{d}S_v$, is independent of the distribution of T_i.

Alternatively, a vertical eccentric limit load can be described as the total force applied at the center of a footing, P, and a moment, M. The work rate of the limit load can then be expressed as the sum of the work rate of the total force, P, and the work rate of the moment, M. For a translational mechanism the moment work rate is, of course, zero. The mechanism must involve footing rotation for the solution to be dependent on the load eccentricity. Meyerhof's hypothesis, however, suggests that the classical Prandtl–Reissner solution be used for eccentric loads, but with footing width reduced by $2e = 2M/P$. While intuitively understandable, this hypothesis is examined here in terms of limit analysis.

A collapse mechanism for a smooth strip footing, with footing rotation, is presented in the next section, and it is shown that the effective width rule is equivalent to assuming the footing smooth in the limit analysis. Next, a mechanism for a rough footing is presented, to indicate the consequences of the effective width rule.

2. Eccentric limit loads on smooth footings

The purpose of this analysis is to show that Meyerhof's effective width hypothesis yields the same bearing capacity as the kinematic approach of limit analysis, which includes footing rotation and a smooth soil-footing interface. This is demonstrated here through closed-form solutions to the problem of bearing capacity of footings

for both cohesive and frictional soils. A comprehensive study of the bearing capacity of strip footings on cohesive (frictionless) soils was carried out recently by Salençon and Pecker [5,6].

A kinematically admissible mechanism of failure of a smooth footing over a frictionless soil is presented in Fig. 1(a). This mechanism is similar to one of those considered by Salençon and Pecker [5]. The footing is loaded with an eccentric vertical load, P, and it rotates during failure about point O with the angular velocity $\dot{\omega}$. Point O is located somewhere along interface AB, but its precise location is yet unknown. This is an incipient mechanism, and the tendency to deform is shown in Fig. 1(b). There is no friction or adhesion (or suction) at the interface, and no internal work needs to be expended if part of the footing separates from the soil surface. The part of the footing width which remains in contact with the soil is denoted by ξB, where coefficient ξ is not known a priori. Region OCB undergoes simple shear, and so does area BDE. Region BCD is subjected to continuous shear. Line $OCDE$ is a strain-rate discontinuity, but not a velocity discontinuity. Notice that the soil along OB undergoes extension, therefore sliding must occur on footing–soil interface OB. Since the footing is assumed to be smooth, this sliding occurs without energy expenditure. The specific terms for the rate of work dissipation and the rate of work of external forces are derived in Appendix A.

Equating the sum of dissipation from expressions in Eqs. (A3), (A4), and (A9), to the work rate of the limit load and the surcharge load in Eqs. (A10) and (A11), one obtains the upper bound solution for the average bearing pressure $\overline{p}$

$$\overline{p} = \frac{1}{2}\,\frac{\xi^2}{\xi + \frac{e}{B} - \frac{1}{2}}\left\{\left[\frac{1}{\tan\alpha} + 2\psi + \frac{1}{\tan(\psi - \alpha)}\right]c + q\right\} \tag{2}$$

where c is the cohesion, and q is the surcharge load. Notice that ξ and angles α and ψ have not been specified, and they will now be found by requiring that $\overline{p}$ in Eq. (2) is the minimum solution (best upper bound), i.e.

$$\frac{\partial \overline{p}}{\partial \alpha} = 0, \qquad \frac{\partial \overline{p}}{\partial \psi} = 0, \qquad \frac{\partial \overline{p}}{\partial \xi} = 0 \tag{3}$$

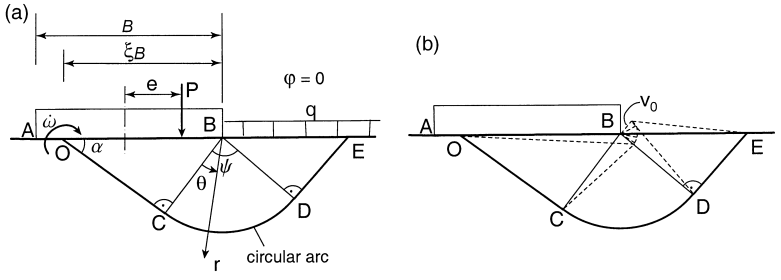

Fig. 1. Collapse mechanism of a cohesive soil under a smooth footing: (a) mechanism with footing rotation and simple shear under the footing, and (b) schematic of the deformed configuration.

The first expression in (3) yields $\psi = 2\alpha$, and the second, one $\psi - \alpha = \pi/4$ (thus, $\alpha = \pi/4$ and $\psi = \pi/2$). Substituting these into Eq. (2), one obtains

$$\overline{p} = [c(2+\pi) + q]\frac{1}{2}\ \frac{\xi^2}{\xi + \frac{e}{B} - \frac{1}{2}} \tag{4}$$

Using the third condition in Eq. (3) yields $\xi = 1 - 2e/B$, hence

$$\overline{p} = [c(2+\pi) + q]\left(1 - 2\frac{e}{B}\right) \tag{5}$$

The expression in Eq. (5) represents the average limit load on a footing subjected to eccentric loading. Although the weight of the soil was not considered, this result is valid for both weightless soil and soil with $\gamma > 0$. This is so because the total work rate of the weight of an incompressible soil with a horizontal surface is equal to zero (a direct consequence of the mass conservation principle in the absence of volumetric strain).

The first part of Eq. (5) $[c(2+\pi) + q]$ is the same as the exact solution to the bearing capacity of a cohesive soil loaded by a centrally applied load. The expression in the second set of parentheses on the right-hand side of Eq. (5) is identical to Meyerhof's procedure of reducing the width of the footing by twice-the-eccentricity. Hence this specific example ($\psi = 0$) shows that Meyerhof's suggestion is equivalent to assuming that the footing is smooth.

An identical conclusion can be drawn for a frictional soil, although the analytic derivation is slightly more elaborate. A closed-form solution, based on the collapse mechanism in Fig. 2, is shown here for a weightless soil. Specific terms for the rate of dissipation and the rate of work of external forces are given in Appendix B. When substituted into Eq. (1), the following expression results for the upper bound to the average bearing pressure

$$\overline{p} = \left\{ c\left[\frac{1}{\tan(\alpha-\varphi)} + \frac{\sin\alpha}{\sin\varphi\sin(\alpha-\varphi)}(e^{2\psi\tan\varphi} - 1) + \frac{\sin\alpha\cos(\psi-\alpha+\varphi)}{\sin(\alpha-\varphi)\sin(\psi-\alpha)} e^{2\psi\tan\varphi} \right] - q\frac{\sin\alpha\sin(\psi-\alpha+\varphi)}{\sin(\alpha-\psi)\sin(\alpha-\varphi)} e^{2\psi\tan\varphi} \right\} \frac{1}{2}\ \frac{\xi^2}{\xi - \frac{1}{2} + \frac{e}{B}} \tag{6}$$

The minimum of $\overline{p}$ is now sought by means of the conditions in Eq. (3), which leads to: $\alpha = \pi/4 + \varphi/2$, $\psi = \pi/2$, and $\xi = 1 - 2e/B$. These, when substituted into Eq. (6), yield

$$\overline{p} = \left(cN_c + qN_q\right)\left(1 - 2\frac{e}{B}\right) \tag{7}$$

where

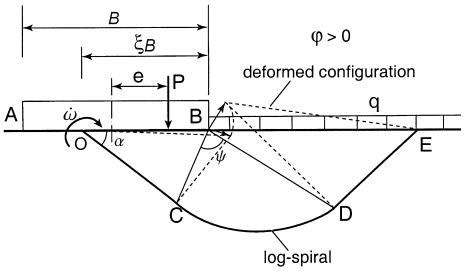

Fig. 2. Failure mechanism of a smooth footing over cohesive-frictional soil (footing rotation, simple shear under the footing).

$$N_c = (N_q - 1)\cot\varphi, \qquad N_q = \tan^2\left(\frac{\pi}{4} + \frac{\varphi}{2}\right)e^{\pi\tan\varphi} \tag{8}$$

The reader will recognize the classical bearing capacity coefficients in Eq. (8) (Prandtl [1], Reissner [2]). It is apparent that for both types of model soils ($\varphi = 0$ and $\varphi > 0$, and $\gamma = 0$) Meyerhof's hypothesis of effective width is equivalent to the limit analysis solution for a smooth footing.

The mechanisms considered in this section allowed for sliding along the footing–soil interface, but this sliding required no energy expenditure, since the footings were considered smooth. It is a straightforward conjecture that for rough footings the average bearing pressure must be larger than that in Eq. (5) or (7), because of the additional internal work that needs to be expended on the interface sliding during failure.

3. Eccentric limit loads on rough footings

A solution to an eccentric limit load on a rough footing is presented in this section, so that a conclusion can be drawn as to the consequences of the effective width rule for realistic (rough) footings.

The mechanism considered here for rough footings does not involve sliding at the footing–soil interface; instead, the footing and the soil immediately underneath rotate as one rigid block. First, a solution will be presented for a frictionless soil. The mechanism considered is presented in Fig. 3(a), and it is similar to the one analyzed earlier by Murff and Miller [7], and more recently by Salençon and Pecker [4,5]. The reader will find a comprehensive analysis of this mechanism in Ref. [5] where the footing is loaded both with an eccentric load and a horizontal force component. The numerical limit analysis approach to the problem of combined loading on strip footings on clay was considered recently by Ukritchon et al. [8]

The footing and area $A'CB$ rotate as one rigid body about point O. The soil in region BCD undergoes shear, with B being a singular point, and block BDE undergoes a superimposed rigid displacement and simple shear. The weight of the soil does not influence the bearing capacity for the frictionless soil, and, for simplicity,

we first consider a case where the surcharge load $q = 0$. The dissipation rate terms for this mechanism are listed in Appendix C. Substituting Eqs. (A10) and (C1) into (1), one obtains the upper bound to the bearing pressure, $\overline{p}$, in the following form

$$\overline{p} = \frac{1}{2}\,\frac{\xi^2}{\xi + \frac{e}{B} - \frac{1}{2}}[(\pi - 2\alpha)\tan^2\alpha + 2\psi - \tan(\psi + \alpha)]c \tag{9}$$

where c is the cohesion, and α, ψ, and ξ are shown in Fig. 3(a). Now, assume that the footing does not separate from the soil, i.e. $\xi = 1$. Using the second condition in Eq. (3), one finds $\psi = 3/4\,\pi - \alpha$, and the first of the conditions in Eq. (3) yields a numerical solution $\alpha = 23.218°$. Substitution into Eq. (9) yields

$$\overline{p} = 5.331c\,\frac{1}{1 + 2\frac{e}{B}} \tag{10}$$

If the third condition in Eq. (3) is used, one finds that the minimum bearing capacity (least upper bound) occurs when the footing separates from the soil, $\xi = 1 - 2e/B$, and the bearing capacity formula becomes

$$\overline{p} = 5.331c\left(1 - 2\frac{e}{B}\right) = cN_c\left(1 - 2\frac{e}{B}\right) \tag{11}$$

While coefficient $(1 - 2e/B)$ is identical to that used by Meyerhof, the bearing capacity factor for the rotational mechanism ($N_c = 5.331$) is slightly larger than that from the classical solution [$Nc = (2+\pi)$]. For small values of e/B ($e/B < 0.065$) the

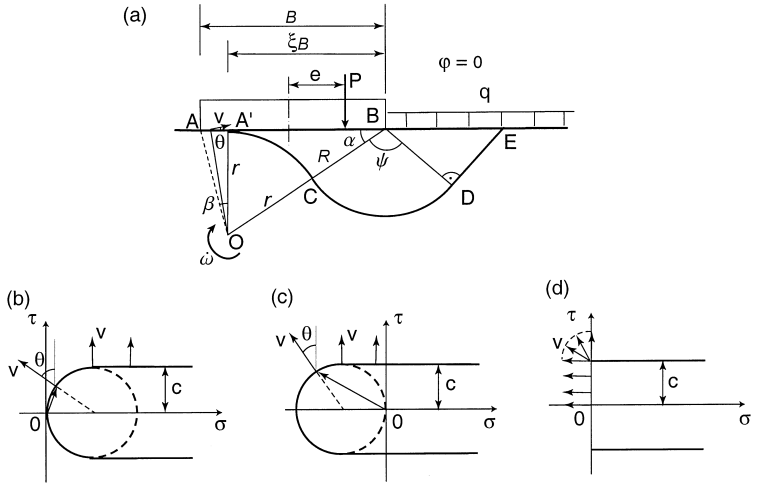

Fig. 3. Rotational collapse of a rough footing over cohesive soil: (a) failure mechanism with soil-footing separation, (b) tension cut-off interface strength model, (c) perfect adhesion interface, and (d) perfectly rough interface model.

mechanism in Fig. 3(a) was substituted with one where $\xi = 1$ and $\beta < 0$ [positive β being shown in Fig. 3(a); notice that when $\xi < 1$, β and ξ are not independent parameters]. Calculations based on such a mechanism lead to a better upper bound on $\overline{p}$ for small e/B, and for the particular case of $e/B = 0$ one obtains $\overline{p} = c(2 + \pi)$—a slight improvement over the solution in Eq. (11).

It was assumed in the derivation of Eq. (11) that no energy is needed to separate the footing from the ground. However, one should expect that for a rough interface, or an interface with some adhesion (or 'suction'), there will be an expenditure of energy for the work needed to debond the footing from the soil. Therefore, we now assume three types of interface:

1. an interface with a tension cut-off according to Fig. 3(b),
2. an interface with perfect adhesion, Fig. 3(c),
3. a perfectly rough interface but with no tensile strength, Fig. 3(d).

The last type of interface was considered by Salençon and Pecker [5]. Velocity vectors marked in Fig. 3(b–d) represent possible separation velocities on interface AA' [Fig. 3(a)]. The term on the left-hand side of Eq. (1) now needs to include an additional energy dissipation rate due to plastic work of the interface debonding process. This additional term, for the three interface models in Fig. 3(b–d), is given in Appendix C.

The solutions to the bearing pressure for footings with rough or adhesive interfaces could be conveniently presented in a form similar to that in Eq. (11), but with a different bearing capacity factor N_c. Since the energy dissipation rate related to the interface separation depends on the distance to which the footing separates from the soil, the bearing capacity factor becomes a function of eccentricity.

4. Numerical results

All the solutions discussed for rough footings over cohesive soils are presented in Fig. 4. The average bearing pressure p is normalized by the classical solution to the bearing pressure of symmetrically loaded footing $\overline{p}_0 = (2 + \pi)c$. The assumption that the footing does not separate from the foundation soil is a significant constraint on the failure mechanism, which results in a bearing pressure significantly larger than that from other solutions. The strength of the soil–footing interface influences the bearing capacity significantly when $e/B > 0.1$. This influence increases with an increase in eccentricity. A soil–footing interface with perfect adhesion [Fig. 3(c)] leads to the second largest bearing pressure. The bearing pressure for both the no-separation and perfect adhesion models approach well-defined, larger-than-zero limits when $e/B \to 0.5$. The tension cut-off and the perfectly rough interface models yield solutions that are no more than 7% and 10% higher, respectively, than that for a smooth footing. The tension cut-off model of the interface is probably a conservative estimate of the interface strength, but a reasonable one for design purposes. Meyerhof's rule then seems to be a reasonable approximation for cohesive soils.

Notice that for a very small eccentricity ($e/B < 0.05$) the rotational mechanism yields the same bearing pressure, no matter what the interface model. This is because, for a small eccentricity, the footing does not separate from the soil, and the energy expenditure for soil–footing separation equals zero, independent of the interface models considered. For a zero eccentricity the best upper bound from the mechanism in Fig. 3(a) is obtained when angle α tends to $\pi/4$ and the center of rotation O moves to infinity. This mechanism then reduces to a classical translation mechanism with region ABC moving as a rigid block.

Results from calculations with a surcharge load are not shown here, but they follow the same trend as those in Fig. 4.

Calculations also have been performed for frictional soils. The rotational mechanism for a frictional soil is shown in Fig. 5, along with two interface models considered. A similar mechanism was considered recently by Paolucci and Pecker [9] in the context of seismic loads. No closed-form solutions were found for cohesive-frictional soils, and the results are presented in a graphical manner in Fig. 6. For simplicity, the soil was first taken as weightless and the surcharge load $q = 0$. The interface friction angle φ_w was taken in computations as equal to the internal friction angle of the soil φ. The solutions follow a trend similar to that for frictionless soil, but the difference between the bearing pressure of a footing with a perfect adhesion interface and a smooth footing decreases now with an increase in the internal friction angle. Numerical calculations shown in Figs. 4 and 6 were all performed for a weightless soil ($\gamma = 0$). The soil weight does not influence the bearing capacity of a frictionless soil since the rate of net work of the soil weight in mechanisms in Figs. 1 and 3 is equal to zero. However, the bearing capacity of frictional soils is affected by γ. The bearing capacity of a footing over a frictional or cohesive-frictional soil varies now depending on cohesion c and surcharge load q. Results of numerical calculations for a variety of model soils and a tension cut-off footing–soil interface

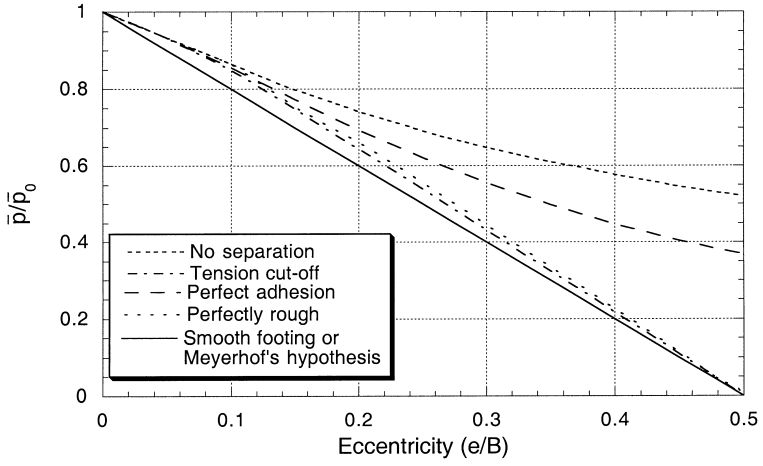

Fig. 4. Solutions to bearing pressure $\bar{p}$ on cohesive soil for different soil–footing interface models (no surcharge).

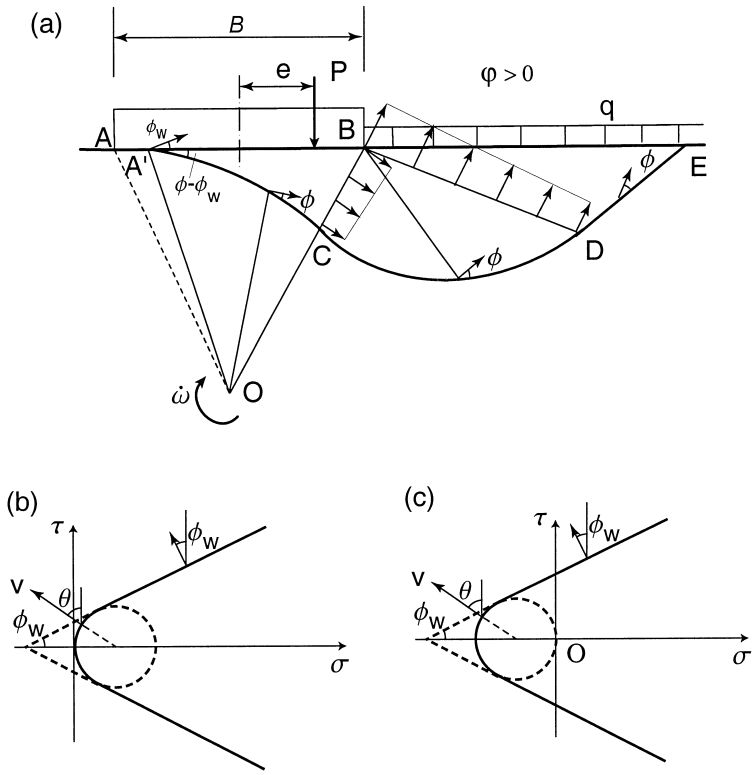

Fig. 5. Rotational failure of a rough footing over cohesive–frictional soil: (a) collapse mechanism, (b) tension cut-off interface model, and (c) perfect adhesion interface.

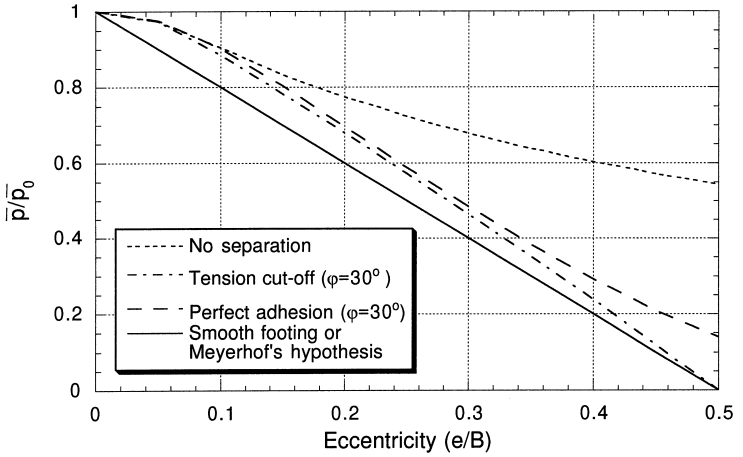

Fig. 6. Solutions to bearing pressure $\bar{p}$ on cohesive–frictional soil for different soil-footing interface models (weightless soil, no surcharge).

[Fig. 5(b)] are presented in Fig. 7. Soils are characterized by their internal friction angle and dimensionless coefficient $c/\gamma B$, and the overburden pressure is given as $q/\gamma B$. Results are normalized by bearing pressure $\overline{p}_0$ of a symmetrically loaded footing ($e/B = 0$). Bearing pressure $\overline{p}_0$ varies now depending on $c/\gamma B$ and $q/\gamma B$. For a frictional-cohesive soil the results follow the same trend as for the cohesive soil, and the effective width rule underestimates the best upper bound solution by about the same margin (8%) as in the case of cohesive soil. However, for purely frictional (granular) soil and relatively small surcharge loads, the effective width rule overestimates the best upper bound to the average bearing pressure. For a surface footing and eccentricity $e/B = 0.25$ this overestimation is 35%, and it increases with an increase in e/B. Fig. 8 presents selected results in a slightly different form, where the failure criterion for an eccentrically loaded footing is shown on the moment–force plane. A straight line drawn through the origin of the M,P coordinate system marks points of equal eccentricity e/B.

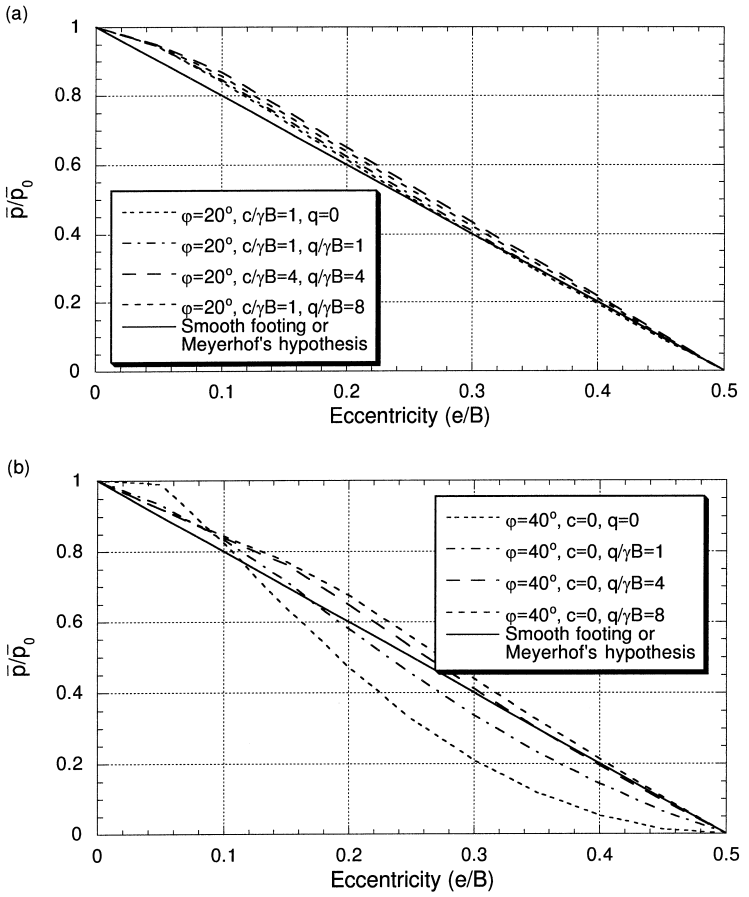

Fig. 7. Numerical solutions to bearing pressure of eccentrically loaded footings (tension cut-off interface).

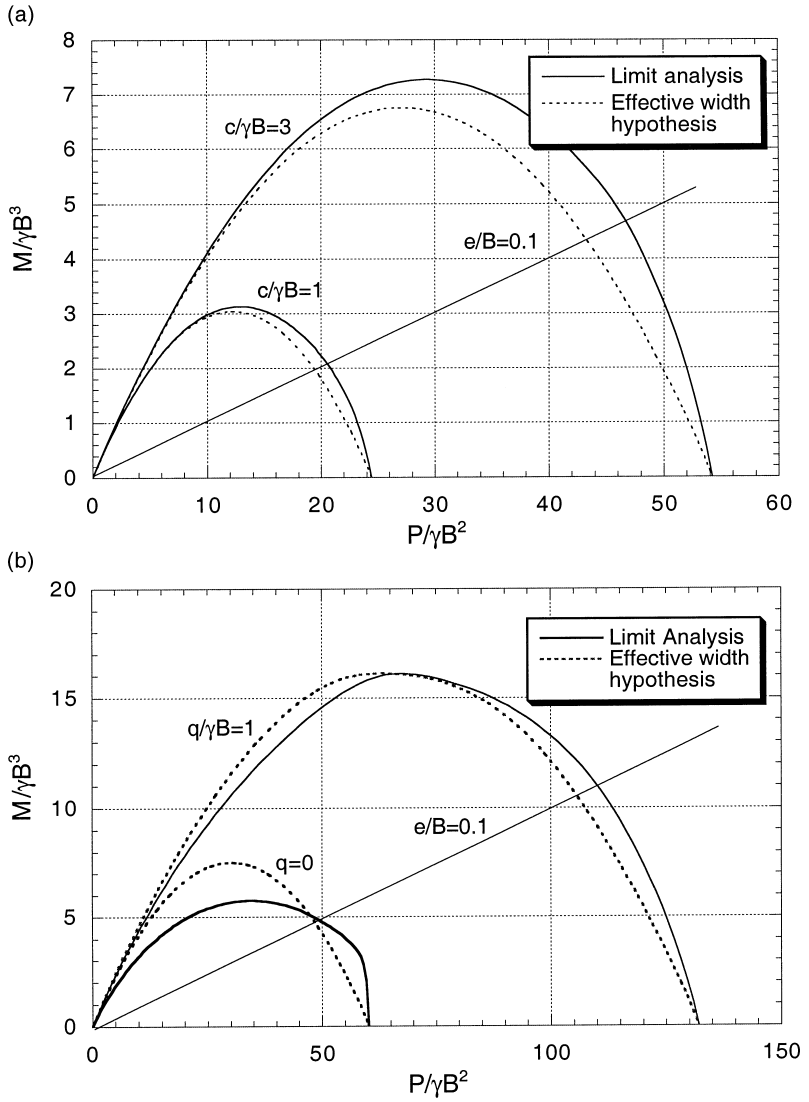

Fig. 8. Failure criteria for shallow footings on the force-moment plane: (a) $\varphi = 20°, q/\gamma B = 1$ and (b) $\varphi = 40°, c = 0$.

Results of calculations with a perfect adhesion interface are shown in Fig. 9. For a relatively small eccentricity ($e/B \leq 0.2$) the trend is similar to that for the tension cut-off interface. For large eccentricities and small internal friction angles, however, the best upper bound to the bearing capacity is considerably larger than that resulting from the effective width rule. This difference decreases with an increase in the internal friction angle.

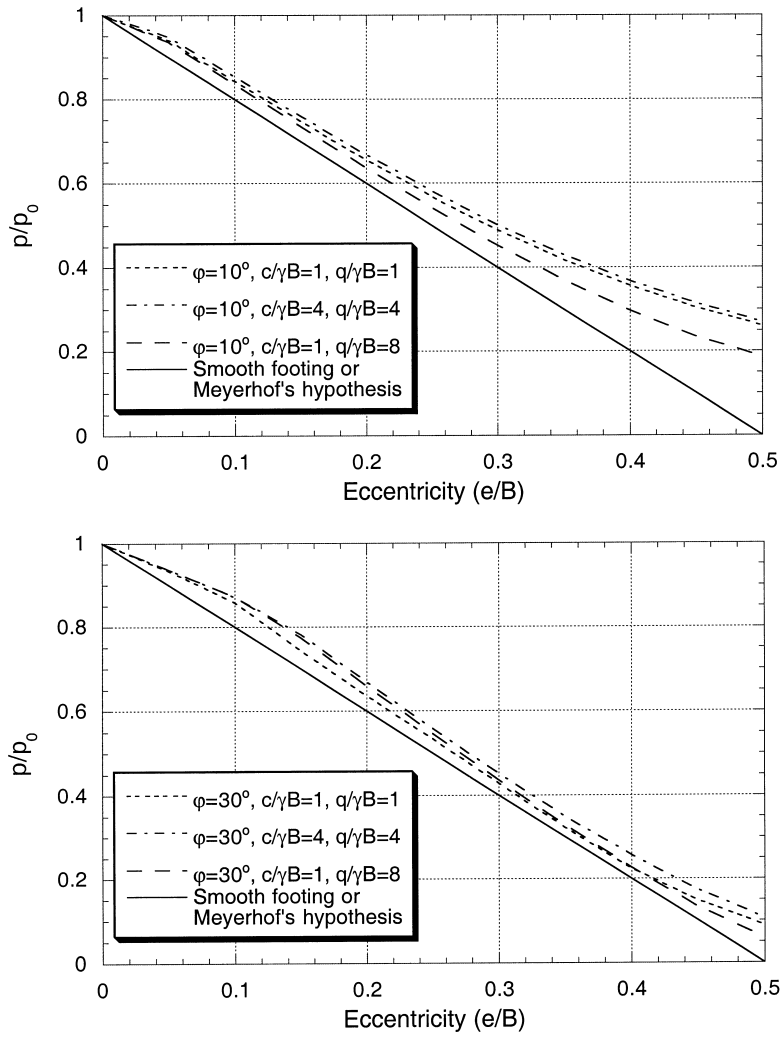

Fig. 9. Numerical solutions to bearing pressure of eccentrically loaded footings (adhesion interface).

5. Final remarks

Eccentric loading on footings is usually considered in calculations of bearing capacity by reducing the size of the footing by twice-the-eccentricity to its 'effective' width. Such a method was first suggested by Meyerhof [3], and it was referred to here as Meyerhof's rule of effective width. It was demonstrated in this paper that this rule leads to the same bearing capacity as the limit analysis solution for a smooth footing, and it underestimates the bearing capacity of footings on cohesive soils with frictional or adhesive soil–footing interfaces. This confirms earlier findings by Salençon and Pecker [5]. The effective width rule significantly underestimates the

bearing capacity for clays ($\varphi \approx 0$) only when the footing is bonded with the soil and the eccentricity is relatively large ($e/B > 0.25$). For cohesive–frictional soils this underestimation decreases with an increase in the internal friction angle. The rule of effective width gives very reasonable estimates of the bearing capacity of eccentrically loaded footings on cohesive or cohesive–frictional soils when the soil–footing interface is not bonded (tension cut-off interface), and for any type of interface when the eccentricity is small ($e/B < 0.1$). In these cases the effective width rule underestimates the best upper bound solution by a margin of no more than 8%. However, it overestimates the bearing capacity for purely frictional soils when the surcharge load is relatively small.

Design codes usually limit the extent of allowable eccentricity. Hence, very significant underestimations and overestimations of bearing capacity, associated with the use of the effective width rule for large eccentricities, are often excluded from practice by design codes.

Acknowledgements

The work presented in this paper was sponsored by the National Science Foundation, grant No. CMS-9634193. This support is greatly appreciated.

Appendix A. Work rate terms for the mechanism with a smooth footing over cohesive soil

The terms for the rates of internal and external work are given here for the analysis based on the mechanism in Fig. 1(a). The soil in region OCB undergoes simple shear [Fig. 1(b)], and the work dissipation rate per unit area in region OCB is calculated from

$$\dot{d} = \sigma_x \dot{\varepsilon}_x + \sigma_y \dot{\varepsilon}_y + \tau_{xy} \dot{\gamma}_{xy} \tag{A1}$$

Assuming axis x for region OCB to coincide with OC, and noting that the deformation for the frictionless material is incompressible, the first two terms in Eq. (A1) are zero, and

$$\dot{d} = c \frac{v_0}{\xi B \sin\alpha} = c \frac{\dot{\omega}}{\sin^2 \alpha} \tag{A2}$$

where v_0 is the magnitude of velocity of point B ($v_0 = \xi B \dot{\omega} / \sin\alpha$), c is the soil cohesion, and angle α is shown in Fig. 1(a), but it is not yet specified. Since the work dissipation rate per unit area is uniform in a simple shear field, the total work dissipation rate in OCB becomes

$$\dot{D}_{OCB} = S_{OCB}\dot{d} = \frac{1}{2}c\dot{\omega}\xi^2 B^2 \cot\alpha \tag{A3}$$

where S_{OCB} is the area of region OCB. Similarly, the work dissipation rate in BDE can be derived as

$$\dot{D}_{BDE} = \frac{1}{2}c\dot{\omega}\xi^2 B^2 \cot(\psi - \alpha) \tag{A4}$$

The deformation pattern in BCD is not a simple shear, and the derivation of the energy dissipation rate is more elaborate. For an incompressible frictionless soil the rate of work dissipation per unit volume undergoing plane deformation is (see, for instance, Davis [10])

$$\dot{d} = (\dot{\varepsilon}_1 - \dot{\varepsilon}_3)c \tag{A5}$$

where $\dot{\varepsilon}_1$ and $\dot{\varepsilon}_3$ are the major and minor principal strain rates, respectively. Introducing polar coordinate system r, θ with the origin at point B, velocities in region BCD can be described as

$$v_r = 0, \quad v_\theta = v_o\left(1 - \frac{r}{R}\right) \tag{A6}$$

where R is the radus of area BCD [see Eq. (A2) for v_0], and the strain rates in region BCD are

$$\begin{aligned}
\dot{\varepsilon}_{rr} &= -\frac{\partial v_r}{\partial r} = 0 \\
\dot{\varepsilon}_{\theta\theta} &= -\frac{1}{r}\frac{\partial v_\theta}{\partial \theta} - \frac{v_r}{r} = 0 \\
\dot{\varepsilon}_{r\theta} &= -\frac{1}{2}\left(\frac{1}{2}\frac{\partial v_r}{\partial \theta} + \frac{\partial v_\theta}{\partial r} - \frac{v_\theta}{r}\right) = \frac{v_0}{2r}
\end{aligned} \tag{A7}$$

The principal strain rates can be calculated easily based on Eq. (A7) as $\dot{\varepsilon}_1 = +\dot{\varepsilon}_{r\theta}$ and $\dot{\varepsilon}_3 = -\dot{\varepsilon}_{r\theta}$, and, using Eq. (A5) the rate of work dissipation per unit volume becomes

$$\dot{d} = c\frac{v_0}{r} = c\frac{\xi B\dot{\omega}}{r\sin\alpha} \tag{A8}$$

and the total energy dissipation rate in region BCD is

$$\dot{D}_{BCD} = \int_0^R \int_0^\psi \dot{d}r\mathrm{d}\theta\mathrm{d}r = c\xi^2 B^2 \dot{\omega}\psi \tag{A9}$$

where $R = \overline{BC}$ [Fig. 1(a)]. The rate of work of the limit load is

$$\dot{W}_p = \overline{p}B^2\dot{\omega}\left(\xi + \frac{e}{B} - \frac{1}{2}\right) \tag{A10}$$

where $\overline{p}$ is the average pressure under the footing ($\overline{p} = P/B$), and the rate of work of overburden pressures is

$$\dot{W}_q = -\frac{1}{2}q\xi^2B^2\dot{\omega} \tag{A11}$$

The respective terms for the work dissipation rate and the rate of external forces now can be substituted into Eq. (1) in order to obtain the expression in Eq. (2) for the upper bound to the bearing pressure $\overline{p}$.

Appendix B. Work rate terms for the mechanism with a smooth footing over frictional soil

Regions OCB and BDE (Fig. 2) undergo simple shear during incipient failure, but, since the material is now frictional, the material dilates. Line CD is now a sector of a log-spiral, and the magnitude of the velocity vector at singular point B is now increasing according to

$$v = v_0 e^{\theta \tan\varphi} \tag{B1}$$

where $v_0 = \xi B\dot{\omega}/\sin(\alpha - \varphi)$, and θ is an angle measured counterclockwise from BC ($0 \le \theta \le \psi$) [Fig. 1(a)]. Following a consideration similar to that in Appendix A, one obtains the following expressions for the work dissipation rates in regions OCB and BDE

$$\dot{D}_{OCB} = \frac{1}{2}c\dot{\omega}\xi^2B^2\cot(\alpha - \varphi) \tag{B2}$$

and

$$\dot{D}_{BDE} = \frac{1}{2}c\dot{\omega}\xi^2B^2\frac{\sin\alpha\cos(\psi - \alpha + \varphi)}{\sin(\alpha - \varphi)\sin(\psi - \alpha)}e^{2\psi\tan\varphi} \tag{B3}$$

The rate of internal work per unit volume of cohesive-frictional soil is

$$\dot{d} = (\dot{\varepsilon}_1 - \dot{\varepsilon}_3)c\cos\varphi \tag{B4}$$

and the total energy dissipation rate in BCD is

$$\dot{D}_{BCD} = \int_0^R \int_0^{\psi} \dot{d}\, r \mathrm{d}\theta \mathrm{d}r = \frac{1}{2} c\xi^2 B^2 \dot{\omega} \frac{e^{2\psi \tan\varphi} - 1}{\sin\varphi \sin(\alpha - \varphi)} \sin\alpha \tag{B5}$$

where $R = \overline{BC} \exp(\theta \tan\varphi)$. The form of $\dot{\mathrm{d}}$ in Eq. (B5) is more complex than that for the cohesive soil in Eq. (A8), because $\dot{\varepsilon}_{\theta\theta}$ in region BCD [Eq. (A7)] is no longer zero. Alternatively, the total dissipation in BCD can be derived by calculating dissipation for an infinitesimal triangle with angle $d\theta$, and integrating it over entire ψ. The rate of work of bearing pressure $\overline{p}$ is

$$\dot{W}_p = \overline{p} B^2 \dot{\omega} \ \ (\xi + \frac{e}{B} - \frac{1}{2}) \tag{B6}$$

and the work rate of the surcharge pressure can be written as

$$\dot{W}_q = -\frac{1}{2} q\xi^2 B^2 \dot{\omega} \frac{\sin\alpha \sin(\psi - \alpha + \varphi)}{\sin(\alpha - \varphi)\sin(\alpha - \psi)} e^{2\psi \tan\varphi} \tag{B7}$$

The terms above, substituted into Eq. (1), yield the expression in Eq. (6).

Appendix C. Work rate terms—rough footing over cohesive soil

The work of limit force P acting at eccentricity e [Fig. 3(a)] is expressed by Eq. (A10), and the respective terms for the work dissipation rate are

$$\begin{aligned} \dot{D}_{A'C} &= 2cr^2(\pi - 2\alpha)\dot{\omega}, \\ \dot{D}_{BCD} &= cR(R + 2r)\psi\dot{\omega} \\ \dot{D}_{BDE} &= -\frac{1}{2} cR(R + 2r)\tan(\alpha + \psi)\dot{\omega} \end{aligned} \tag{C1}$$

The dissipation rates for regions BCD and BDE include the dissipation within the continually deforming soil, and along the discontinuity segments CD and DE, respectively.

The energy dissipation rate per unit length of the interface described by the tension cut-off and the perfect adhesion models is

$$\dot{d} = cv(1 \mp \sin\theta) \tag{C2}$$

where v and θ are the velocity at the interface and its inclination angle, respectively [see Fig. 3(a–c)]. The total energy dissipation at the interface is

$$\dot{D}_{AA'} = \int_0^{\beta} \dot{d}\frac{r\mathrm{d}\theta}{\cos^2\theta} = \frac{1}{2}c\dot{\omega}B^2\xi^2\tan^2\alpha\left\{\frac{\sin\beta}{1\pm\sin\beta} + \ln\left[\tan\left(\frac{\pi}{4}+\frac{\beta}{2}\right)\right]\right\} \tag{C3}$$

where

$$\tan\beta = \frac{1-\xi}{\xi\tan\alpha} \tag{C4}$$

The top and bottom signs in Eqs. (C2) and (C3) relate to the tension cut-off [Fig. 3(b)] and perfect adhesion [Fig. 3(c)) interfaces, respectively.

The energy dissipation rate at the perfectly rough interface [Fig. 3(d)] is

$$\dot{D}_{AA'} = \int_0^{\beta} cr\dot{\omega}\frac{r\mathrm{d}\theta}{\cos^2\theta} = c\dot{\omega}B^2\xi(1-\xi)\tan\alpha. \tag{C5}$$

References

[1] Prandtl L. Über die Härte plastischer Körper. Nachr Ges Wissensch, Göttingen, math.-phys. Klasse 1920;74–85.

[2] Reissner H. Zum Erddruckproblem. In: Proceedings, First Int. Congress for Applied Mechanics,. Buezeno CB, Burgers JM, editors. Delft; JR Waltman 1924:295–311.

[3] Meyerhof GG. The bearing capacity of foundations under eccentric and inclined loads. In: 3rd ICSMFE Vol. 1. Zürich: 1953:440–45.

[4] Pecker A, Salençon J. Seismic bearing capacity of shallow strip foundations on clay soils. In: Proc International Workshop on Seismology and Earthquake Engineering. Mexico: 1991:116–34.

[5] Salençon J, Pecker A. Ultimate bearing capacity of shallow foundations under inclined and eccentric loads. Part I: purely cohesive soil. Eur J Mech A/Solids 1995;14(3):249–75.

[6] Salençon J, Pecker A. Ultimate bearing capacity of shallow foundations under inclined and eccentric loads. Part II: purely cohesive soil without tensile strength. Eur J Mech A/Solids 1995;14(3):377–96.

[7] Murff JD, Miller TW. Foundation stability on nonhomogeneous clays. J Geotech Eng Div 1977;103(10):1083–97.

[8] Ukritchon B, Whittle A, Sloan SW. Undrained limit analysis for combined loading of strip footing on clay. Geotechn Geoenv Engrg 1998;124(3):265–76.

[9] Paolucci R, Pecker A. Seismic bearing capacity of shallow strip foundations on dry soils. Soils and Foundations 1997;37(3):95–105.

[10] Davis EH. Theories of plasticity and the failure of soil masses. In: Soil Mechanics: Selected Topics, Lee IK, editor. London: Butterworth, 1968:341–80.